JOURNAL OF RESEARCH of the National Bureau of Standards—D. Radio Propagation
Vol. 66D, No. 6, November–December 1962

Very-Low-Frequency Radio Propagation in the Ionosphere

Daniel W. Swift

Contribution from Research and Advanced Development Division, Avco Corporation, Wilmington, Mass.

(Received April 27, 1962; revised June 5, 1962)

Equations describing the propagation of radio waves in a horizontally stratified anisotropic ionosphere were developed by considering the limiting case of a large number of infinitesimally thin slabs of constant electron density and collision frequency. The quasi-longitudinal approximation was used. The propagation equations appeared as four coupled first-order linear differential equations, coupled by gradients in electron density and collision frequency. The quasi-longitudinal approximation permitted use of particularly simple forms for the coupling coefficients, these forms being amenable to simple analysis. Coupling between two ordinary or two extraordinary modes was found to be considerably stronger than cross coupling between ordinary and extraordinary modes. Cross coupling was related to the rate of change of the direction of the phase normal. It was found that the reflection of VLF radio waves from the daytime ionosphere is relatively insensitive to the angle of incidence on the ionosphere except for highly oblique propagation. Whistler penetration was also found to be insensitive to the angle of incidence on the ionosphere.

1. Introduction

In this report, we shall consider the full-wave solutions for a very low frequency radio wave propagating obliquely into a horizontally stratified ionosphere. The effects produced by the presence of the geomagnetic field and by electron collisions will be considered in some detail. Although ionospheric reflection coefficients have been accurately calculated by Johler and Harper [1962] for quite general conditions, the impetus for this study is to understand more fully the reflection processes of VLF radio waves and to understand the penetration of radio waves through the ionosphere. Wait [1960] and Barron and Budden [1959] have conducted extensive investigations of the reflecting properties of the ionosphere using the quasi-longitudinal approximation and the mode theory; however, the actual reflection processes of the ionosphere have not been investigated.

This report will consider the propagation of four separate magneto-ionic modes in a horizontally stratified ionosphere. The quasi-longitudinal approximation will be used in this analysis. The four modes have propagation constants given by the roots of the Booker quartic equation and represent two upward-propagating modes, ordinary and extraordinary, and two similar downward-propagating modes.

The equations for the coupled modes will be developed through consideration of the ionosphere as a series of step functions where, in between the steps, the electron density and collision frequency remain constant. Expressions will be written for the electric field intensity for each of the four modes within each step. These expressions will be related to the electric field intensity of a neighboring slab by means of the boundary conditions. Then the limit is taken as the width of each slab, and the change in electron density and collision frequency across each slab becomes infinitesimally small. Four differential equations are obtained for each mode, and they are coupled by gradients in the electron density and collision frequency.

Although the general full-wave equations for ionospheric radio propagation are known [Budden 1961], they have not been studied in detail for oblique incidence because of the great complexity of the coupling coefficients. However, by using the quasi-longitudinal approxima-

tion, remarkable simplifications can be made which permit the simple analysis of the behavior of VLF radio waves in the ionosphere. Limitations on the quasi-longitudinal approximation will also be discussed.

The reflection processes will be discussed as the coupling of the upgoing modes to the downgoing modes. Explicit representations of this coupling will be given as a function of altitude for a typical daytime ionosphere. The reflectivity of the D region as a function of the angle of incidence will be qualitatively indicated. The penetration of very-low-frequency signals through the ionosphere will also be qualitatively discussed by examining how much of the wave is coupled into the downgoing modes and how much is attenuated when passing through the ionosphere. The optimum conditions for penetration from the ground into the ionosphere will be indicated.

2. Development of the Propagation Equations

2.1. Basic Considerations

In this section we shall begin by showing the equations for a wave propagating in a uniform magneto-ionic medium. We shall then express the boundary conditions for a wave incident upon a plane boundary where a discontinuous change in the propagation constant occurs.

The quasi-longitudinal approximation for the propagation constant is given by

$$k=\frac{1}{c}\left(\omega^2+\frac{\omega\omega_P^2}{-\omega+i\nu\pm\omega_m\cos\theta}\right)^{\frac{1}{2}} \tag{1}$$

where

$\omega=2\pi f$,
$\omega_P^2=\frac{e^2N_e}{\epsilon_0 m}$ (square of the angular plasma frequency),
ν=electron collision frequency,
$\omega_m=\frac{eB_0}{m}$ electron gyrofrequency (ω_m is negative because the electron has a negative charge),
m=electron mass,
e=electron charge,
N_e=ionospheric electron density,
B_0=magnetic induction of the earth's field,
θ=angle between direction of wave normal and direction of the geomagnetic field,
c=velocity of light.

Equation (1) is valid in the limit that [Budden, 1961, p. 119]

$$\frac{\omega_m^2\sin^4\theta}{4\omega^2\cos^2\theta}\left|1-\frac{\omega_P}{\omega}-i\frac{\nu}{\omega}\right|^{-2}<<1. \tag{2}$$

Suffice it to say for the present that (2) holds for VLF propagation provided that θ is not "too near" 90 degrees. Equation (2) will be investigated in more detail later in this paper.

Returning now to (1), we see that because of the presence of a magnetic field through the term ω_m, there are two modes of propagation and the medium is also anisotropic. Let us denote k of (1) as k_1 when the plus sign is used and k_2 when the minus sign is used. We notice that if the conditions of (2) are satisfied and if $\cos\theta>0$, a wave of propagation constant k_1 will generally propagate and a wave of propagation constant k_2 will be heavily damped.

Before writing analytic expressions for the propagating waves, we shall adopt the coordinate system shown in figure 1. The magnetic field B_0 is confined to the x-z plane and is inclined at an angle δ to the x-axis. The electron density and collision frequency is to vary only in the z direction. The direction of propagation is denoted by the vector $\vec{1}_k$ at an angle ψ to the z-axis and with an azimuthal angle ϕ. The unit vector $\vec{1}_k$ is therefore given by

$$\vec{1}_k=\vec{1}_z\cos\psi+(\vec{1}_x\cos\phi+\vec{1}_y\sin\phi)\sin\psi. \tag{3}$$

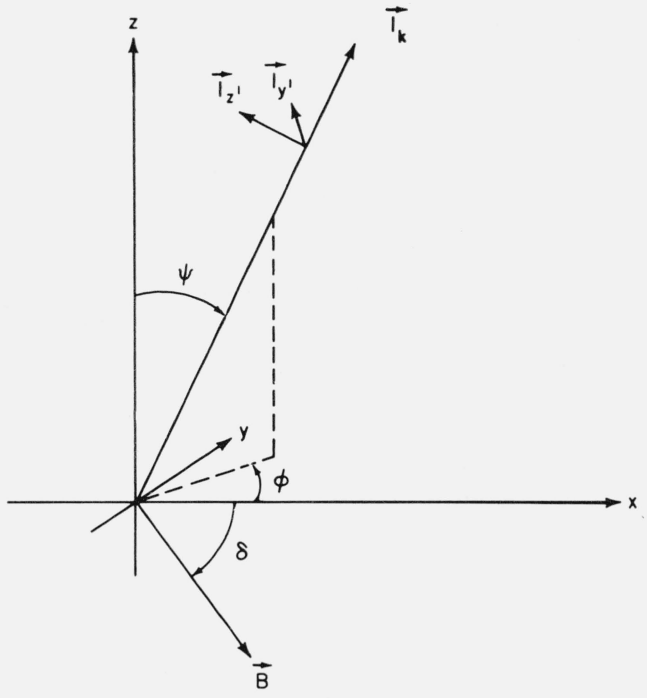

FIGURE 1. *Coordinate system.*

The geomagnetic field vector may be represented by

$$\vec{B}_0 = B_0(-\vec{1}_z \sin\delta + \vec{1}_x \cos\delta). \tag{4}$$

It is now easy to compute $\cos\theta$ in (1). It is given by

$$\cos\theta = -\cos\psi \sin\delta + \sin\psi \cos\delta \cos\phi. \tag{5}$$

In the quasi-longitudinal approximation, mode 1 will be right-handedly circularly polarized and mode 2 will be left-handedly circularly polarized. Let $\vec{1}_{y'}$ and $\vec{1}_{z'}$ be two vectors forming a right-handed orthogonal coordinate set of unit vectors with $\vec{1}_k$. Then, in general, the electric vector of a plane-propagating upgoing wave in a homogeneous medium may be represented by

$$\begin{aligned}\vec{E}^u(x, y, z) = {} & E_1(\vec{1}_{y'} + i\vec{1}_{z'}) \exp\{-ik_1[\cos\psi_1 z + \sin\psi_1(y\sin\phi + x\cos\phi)]\} \\ & + E_2(\vec{1}_{y'} - i\vec{1}_{z'}) \exp\{-ik_2[\cos\psi_2 z + \sin\psi_2(y\sin\phi + x\cos\phi)]\}\end{aligned} \tag{6}$$

where E_1 and E_2 are constants.

Let us further define $\vec{1}_{y'}$ as being parallel to the xy-plane; then

$$\vec{1}_{y'} = \vec{1}_y \cos\phi - \vec{1}_x \sin\phi, \tag{7a}$$

so that $\vec{1}_{z'}$ may be determined; namely,

$$\vec{1}_{z'} = \vec{1}_k \times \vec{1}_{y'} = \vec{1}_z \sin\psi - (\vec{1}_x \sin\phi + \vec{1}_x \cos\phi)\cos\psi. \tag{7b}$$

Therefore, when $\vec{1}_k$ points along the x-axis, then $\vec{1}_{y'}$ is along the y-axis and $\vec{1}_{z'}$ is along the z-axis

2.2. Reflection From a Plane Boundary

When a wave is incident on a boundary between two regions with differing refractive indices, part of the wave will be transmitted across the boundary and part will be reflected. The reflected wave corresponds to two more modes with propagation constants.

$$k=\frac{1}{c}\left[\omega^2+\frac{\omega\,\omega_p^2}{-\omega+i\nu\pm\omega_m\,(\cos\psi\sin\delta+\sin\psi\cos\delta\cos\phi)}\right], \tag{8}$$

where we shall say k_3 is the mode corresponding to the minus sign, and k_4 is the mode corresponding to the plus sign. Equation (8) differs from (1) in that the sign on $\cos\psi$ has been changed. (Wherever $\cos\psi$ or $\sin\psi$ appears, it will always be understood that the real part is positive.)

The electric field of the downward propagating waves is given by

$$\vec{E}^d=E_3(\vec{1}_{y'}+i\vec{1}_{z'})\exp\{ik_3[\cos\psi_3 z+\sin\psi_3\,(y\sin\phi+x\cos\phi)]\}$$
$$+E_4(\vec{1}_{y'}-i\vec{1}_{z'})\exp\{ik_4[\cos\psi_4 z+\sin\psi_4\,(y\sin\phi+x\cos\phi)]\}. \tag{8a}$$

When using this expression, it must be remembered that k_4 is the propagating mode and k_3 is the evanescent mode, under the condition that the sign on the projection of the direction of propagation on the geomagnetic field, $\cos\theta$, has changed from that appearing in the upgoing modes. This will usually be the case for VLF propagation in temperate and polar latitudes. When $\cos\theta$ does not change sign between the incident and reflected modes, mode 4 is evanescent and mode 3 is propagating.

Let us now consider a plane boundary in the x–y plane located at z_i. Let the propagation constant at $z<z_i$ be k_j^i, and at $z>z_i$, k_j^{i+1} where $j=1,2,3,4$, corresponding to the two reflected (downgoing) and two incident or transmitted (upgoing) waves. Further consider another boundary at $z=z_{i+1}$ such that both above and below the boundary at z_i there are two upgoing and two downgoing waves.

The boundary conditions are that the tangential component of $\vec{E}$ and of $\nabla\times\vec{E}$ be continuous across the boundary. Therefore, by equating the x and y components of $\vec{E}$ and $\nabla\times\vec{E}$ we obtain four equations relating E_j^i to E_j^{i+1}. Thus the boundary conditions can be expressed in the form

$$\begin{bmatrix} a_{11}^i & a_{12}^i & a_{13}^i & a_{14}^i \\ a_{21}^i & a_{22}^i & a_{23}^i & a_{24}^i \\ a_{31}^i & a_{33}^i & a_{33}^i & a_{34}^i \\ a_{41}^i & a_{42}^i & a_{43}^i & a_{44}^i \end{bmatrix} \begin{bmatrix} \boldsymbol{E}_1^i \\ \boldsymbol{E}_2^i \\ \boldsymbol{E}_3^i \\ \boldsymbol{E}_4^i \end{bmatrix} = \begin{bmatrix} a_{11}^{i+1} & a_{12}^{i+1} & a_{13}^{i+1} & a_{14}^{i+1} \\ a_{21}^{i+1} & a_{22}^{i+1} & a_{23}^{i+1} & a_{24}^{i+1} \\ a_{31}^{i+1} & a_{32}^{i+1} & a_{33}^{i+1} & a_{34}^{i+1} \\ a_{41}^{i+1} & a_{42}^{i+1} & a_{43}^{i+1} & a_{44}^{i+1} \end{bmatrix} \begin{bmatrix} \boldsymbol{E}_1^{i+1} \\ \boldsymbol{E}_2^{i+1} \\ \boldsymbol{E}_3^{i+1} \\ \boldsymbol{E}_4^{i+1} \end{bmatrix} \tag{9}$$

where

$$\boldsymbol{E}_j^i=E_j^i\exp\{-ik_j^i[\epsilon(j)\cos\psi_j^i z_i+\sin\psi_j^i(x\cos\phi+y\sin\phi)]\},$$

and where

$$\epsilon(1)=1,\ \epsilon(2)=1,\ \epsilon(3)=-1,\ \epsilon(4)=-1.$$

The elements of the square matrices are computed from the x and y components of $(\vec{1}_{y'}\pm i\vec{1}_{z'})$ and from the x and y components

$$\vec{1}_{kj}\times(\vec{1}_{y'}\pm i\vec{1}_{z'})k_j=(\vec{1}_{z'}\mp i\vec{1}_{y'}k_j \tag{10}$$

The matrix elements, a^i_{kj}, may be written

$$a^i_{1j}=-\sin\phi+i(-1)^j\epsilon(j)\cos\phi\cos\psi^i_j \tag{11a}$$

$$a^i_{2j}=\cos\phi+i(-1)^j\epsilon(j)\sin\phi\cos\psi^i_j \tag{11b}$$

$$a^i_{3j}=[-\epsilon(j)\cos\phi\cos\psi^i_j+i(-1)^j\sin\phi]k_j \tag{11c}$$

$$a^i_{4j}=[-\epsilon(j)\sin\phi\cos\psi^i_j-i(-1)^j\cos\phi]k_j. \tag{11d}$$

In order to satisfy the conditions of (9) at any point (x,y) in the $z=z_i$ plane, the auxiliary condition

$$k^i_j\sin\psi^i_j=\frac{\omega}{c}\sin\psi_0 \tag{12}$$

must be satisfied for all values of j and at all levels in the ionosphere where ψ_0 is the zenith angle of the wave below the ionosphere. Thus when an electromagnetic wave enters the ionosphere it will split into four modes, two transmitted and two reflected, all propagating in different directions. However, the azimuthal direction for the phase normals must be the same for all four modes.

The problem of determining the angle ψ_j is by no means trivial because from (1), (5), and (8) it can be seen that k_j is an irrational function of $\sin\psi^i_j$. The solution of (12) for $\sin\psi^i_j$ or $\cos\psi^i_j$ is equivalent to solving the Booker quartic equation for the four roots $k^i_j\cos\psi^i_j$ given the value of $\frac{\omega}{c}\sin\psi_0$. However in practice, a simple iterative solution for $\sin\psi_j$ can be found. For example, if $\sin\psi^i_j$ is known and it is desired to find $\sin\psi^{i+1}_j$ then we let $\sin\psi^{i+1}_{j,l}$ be the lth step in the iterative process described by the equation

$$\sin\psi^{i+1}_{j,l}=\frac{\frac{\omega}{c}\sin\psi_0}{k^{i+1}_j(\sin\psi^{i+1}_{j,l-1})}, \tag{13}$$

where

$$\sin\psi^{i+1}_{j,0}=\sin\psi^i_j.$$

This simple routine will converge in a very few steps.

Returning now to (11) we notice that

$$-a^i_{1j}\sin\phi+a^i_{2j}\cos\phi=1 \tag{14a}$$

$$a^i_{1j}\cos\phi+a^i_{2j}\sin\phi=(-1)^j\epsilon(j)\cos\psi^i_j \tag{14b}$$

$$a^i_{3j}\sin\phi-a^i_{4j}\cos\phi=(-1)^jk^i_j \tag{14c}$$

$$a^i_{3j}\cos\phi+a^i_{4j}\sin\phi=-\epsilon(j)\cos\psi^i_jk^i_j \tag{14d}$$

which results in a considerable simplification over (11), so that (9) may be written in the form

$$\begin{bmatrix} 1 & 1 & 1 & 1 \\ -\cos\psi^i_1 & \cos\psi^i_2 & \cos\psi^i_3 & -\cos\psi^i_4 \\ k^i_1 & -k^i_2 & k^i_3 & -k^i_4 \\ -k^i_1\cos\psi^i_1 & -k^i_2\cos\psi^i_2 & k^i_3\cos\psi^i_3 & k^i_4\cos\psi^i_4 \end{bmatrix}\begin{bmatrix} \boldsymbol{E}^i_1 \\ \boldsymbol{E}^i_2 \\ \boldsymbol{E}^i_3 \\ \boldsymbol{E}^i_4 \end{bmatrix}$$

$$=\begin{bmatrix} 1 & 1 & 1 & 1 \\ -\cos\psi^{i+1}_1 & \cos\psi^{i+1}_2 & \cos\psi^{i+1}_3 & -\cos\psi^{i+1}_4 \\ k^{i+1}_1 & -k^{i+1}_2 & k^{i+1}_3 & -k^{i+1}_4 \\ -k^{i+1}_1\cos\psi^{i+1}_1 & -k^{i+1}_2\cos\psi^{i+1}_2 & k^{i+1}_3\cos\psi^{i+1}_3 & k^{i+1}_4\cos\psi^{i+1}_4 \end{bmatrix}\begin{bmatrix} \boldsymbol{E}^{i+1}_1 \\ \boldsymbol{E}^{i+1}_2 \\ \boldsymbol{E}^{i+1}_3 \\ \boldsymbol{E}^{i+1}_4 \end{bmatrix} \tag{15}$$

where $\boldsymbol{E}^i_j$ is now understood to mean $E^i_j\exp[-i\epsilon(j)k^i_j\cos\psi^i_jz_i]$.

2.3. Transition to the Continuous Ionosphere

In the preceding section, we considered plane waves incident on a sharp boundary between regions of different electron density. Let us now examine a large number of steps which approximate continuous ionospheric conditions in a manner shown in figure 2. Let each of the intervals in figure 2 be of width Δz and let the index "i" in (15) refer to the ith interval. Then the quantities in the $(i+1)$ interval may be represented in terms of the ith interval, provided that the change between the intervals is small, by the relations

$$E_j^{i+1}=E_j^i+\frac{dE_j^i}{dz}\Delta z \tag{16a}$$

$$k_j^{i+1}=k_j^i+\frac{dk_j^i}{dz}\Delta z \tag{16b}$$

$$\cos\psi_j^{i+1}=\cos\psi_j^i+\frac{d}{dz}(\cos\psi_j^i)\Delta z \tag{16c}$$

and

$$\exp\left[-\epsilon(j)ik_j^{i+1}\cos\psi_j^{i+1}z_i\right]=\exp\left[-\epsilon(j)ik_j^i\cos\psi_j^iz_i\right]\times\left[1-i\epsilon(j)\frac{d}{dz}(k_j^i\cos\psi_j^i)z_i\Delta z\right]. \tag{17}$$

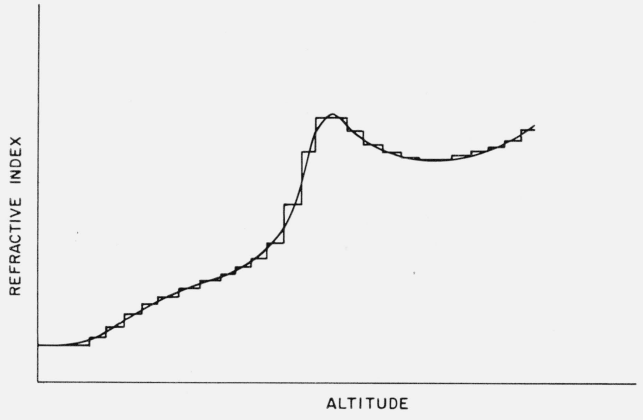

FIGURE 2. *Representation of a continuous ionosphere as a step function.*

Upon combining (16a) and (17) and neglecting terms of order $(\Delta z)^2$ we get

$$\boldsymbol{E}_j^{i+1}=E_j^i\exp\left[-i\epsilon(j)k_j^i\cos\psi_j^iz_i\right]+\exp\left[-i\epsilon(j)k_j^i\cos\psi_j^iz_i\right]\left[-i\epsilon(j)E_j^iz_i\frac{d}{dz}(k_j^i\cos\psi_j^i)+\frac{d}{dz}E_j^i\right]\Delta z,$$

which may be written in the more desirable form,

$$\boldsymbol{E}_j^{i+1}=\boldsymbol{E}_j^i+\left[\frac{d}{dz}\boldsymbol{E}_j^i+i\epsilon(j)\boldsymbol{E}_j^ik_j^i\cos\psi_j^i\right]\Delta z. \tag{18}$$

Upon substituting (16b), (16c), and (18) into (15) and using the variable z instead of the subscripted variable z_i we get a coupled set of differential equations which express the boundary conditions between layers infinitesimal thickness Δz:

$$\begin{bmatrix} 1 & 1 & 1 & 1 \\ -\cos\psi_1 & \cos\psi_2 & \cos\psi_3 & -\cos\psi_4 \\ k_1 & -k_2 & k_3 & -k_4 \\ -k_1\cos\psi_1 & -k_2\cos\psi_2 & k_3\cos\psi_3 & k_4\cos\psi_4 \end{bmatrix} \frac{d}{dz} \begin{bmatrix} \boldsymbol{E}_1 \\ \boldsymbol{E}_2 \\ \boldsymbol{E}_3 \\ \boldsymbol{E}_4 \end{bmatrix}$$

$$= \begin{bmatrix} -ik_1\cos\psi_1 & -ik_2\cos\psi_2 & ik_3\cos\psi_3 & ik_4\cos\psi_4 \\ ik_1\cos^2\psi_1 & -k_2\cos^2\psi_2 & ik_3\cos^2\psi_3 & -k_4\cos^2\psi_4 \\ -ik_1^2\cos\psi_1 & ik_2^2\cos\psi_2 & ik_3^2\cos\psi_3 & -k_4^2\cos\psi_4 \\ ik_1^2\cos\psi_1^2 & ik_2^2\cos\psi_2 & ik_3^2\cos\psi_3 & ik_4^2\cos\psi_4 \end{bmatrix} \begin{bmatrix} \boldsymbol{E}_1 \\ \boldsymbol{E}_2 \\ \boldsymbol{E}_3 \\ \boldsymbol{E}_4 \end{bmatrix}$$

$$-\frac{d}{dz} \begin{bmatrix} 1 & 1 & 1 & 1 \\ -\cos\psi_1 & \cos\psi_2 & \cos\psi_3 & -\cos\psi_4 \\ k_1 & -k_2 & k_3 & -k_4 \\ -k_1\cos\psi_1 & -k_2\cos\psi_2 & k_3\cos\psi_3 & k_4\cos\psi_4 \end{bmatrix} \begin{bmatrix} \boldsymbol{E}_1 \\ \boldsymbol{E}_2 \\ \boldsymbol{E}_3 \\ \boldsymbol{E}_4 \end{bmatrix} \tag{19}$$

This equation is somewhat awkward in that the derivatives of the $\boldsymbol{E}_j$ are mixed. The form of these equations can be considerably simplified if we note that the first term on the right-hand side of (19) can be factored

$$\begin{bmatrix} 1 & 1 & 1 & 1 \\ -\cos\psi_1 & \cos\psi_2 & \cos\psi_3 & -\cos\psi_4 \\ k_1 & -k_2 & k_3 & -k_4 \\ -k_1\cos\psi_1 & -k_2\cos\psi_2 & k_3\cos\psi_3 & k_4\cos\psi_4 \end{bmatrix} \begin{bmatrix} -k_1\cos\psi_1 & 0 & 0 & 0 \\ 0 & -ik_2\cos\psi_2 & 0 & 0 \\ 0 & 0 & ik_3\cos\psi_3 & 0 \\ 0 & 0 & 0 & ik_4\cos\psi_4 \end{bmatrix} = AQ \tag{20}$$

where Q is the diagonal matrix. If we let $\vec{\boldsymbol{E}}$ be the column matrix containing $\boldsymbol{E}_j$ then (19) has the form

$$A\vec{\boldsymbol{E}}' = (AQ - A')\vec{\boldsymbol{E}} \tag{21}$$

where the prime denotes differentiation with respect to z. The form of (21) may be considerably simplified if we multiply through on the left by A^{-1} obtaining

$$\vec{\boldsymbol{E}}' = Q\vec{\boldsymbol{E}} - A^{-1}A'\vec{\boldsymbol{E}}. \tag{22}$$

Since Q of (22) is diagonal, we see that the elements of the matrix $A^{-1}A$ couple the modes together. We further see that coupling is dependent upon gradients in the electron density and collision frequency. If the coupling matrix is small, then all modes propagate almost independently and

$$\boldsymbol{E}_j \cong \exp\left[-i\epsilon(j)\int_0^z k_j\cos\psi_j dz\right]. \tag{23}$$

If we let $(A^{-1})_{ij}$ represent an element of A^{-1}, then the (i, j)th element in the coupling matrix $A^{-1}A = C$ may be written

$$C_{ij} = \epsilon(j)\frac{d}{dz}(\cos\psi_j)[(-1)^j(A^{-1})_{2i} - k_j(A^{-1})_{4i}] - \frac{d}{dz}k_j[(-1)^j(A^{-1})_{3i} + \epsilon(j)\cos\psi_j(A^{-1})_{4i}]. \tag{24}$$

Here we notice that the coupling between modes is produced by gradients in electron density and collision frequency, and also that when the ionosphere is homogeneous, the modes propagate independently with solution given by (23).

3. Coupling Matrix

The coupling coefficients corresponding to the matrix C have been computed by Heading (see Budden [1961]) for the general case corresponding to the full Appleton-Hartree formula without approximation. His expressions for C are quite complicated and difficult to interpret except by computing numerical examples. The use of the quasi-longitudinal approximation permits considerable simplification of the coupling matrix to the point where physical interpretations are possible without making use of detailed computations.

In order to simplify the notation used here, let us write

$$c_j = \cos \psi_j.$$

Then we may begin the computation of c_{ij} by finding the determinant of A, namely

$$|A| = (k_1+k_4)(k_2+k_3)(c_1+c_3)(c_2+c_4) - (k_1-k_3)(k_2-k_4)(c_2-c_3)(c_1-c_4). \tag{25}$$

A^{-1} is then computed by finding the cofactor of A, making use of (25). The elements of C are then found by substituting A^{-1} into (24) and rearranging terms; thus

$$\begin{aligned}|A|C_{11} = {} & c_1'[(k_1+k_4)(k_2+k_3)(c_2+c_4) - (k_1-k_3)(k_2-k_4)(c_2-c_3)] \\ & + k_1'[(k_2+k_3)(c_1+c_3)(c_2+c_4) - (k_2-k_4)(c_1-c_4)(c_2-c_3)]\end{aligned} \tag{26a}$$

$$|A|C_{12} = c_2'(k_2-k_4)(k_2+k_3)(c_3+c_4) + k_2'(k_3+k_4)(c_2-c_3)(c_2+c_4) \tag{26b}$$

$$|A|C_{13} = -c_3'(k_3+k_4)(k_2+k_3)(c_2+c_4) + k_3'(k_2-k_4)(c_2-c_3)(c_3+c_4) \tag{26c}$$

$$|A|C_{14} = c_4'(k_3+k_4)(k_2-k_4)(c_2-c_3) - k_4'(k_2+k_3)(c_2+c_4)(c_3+c_4) \tag{26d}$$

$$|A|C_{21} = c_1'(k_1-k_3)(k_1+k_4)(c_3+c_4) + k_1'(k_3+k_4)(c_1+c_3)(c_1-c_4) \tag{26e}$$

$$\begin{aligned}|A|C_{22} = {} & c_2'[(k_2+k_3)(k_1+k_4)(c_1+c_3) - (k_2-k_4)(k_1-k_3)(c_1-c_4)] \\ & + k_2'[(k_1+k_4)(c_2+c_4)(c_1+c_3) - (k_1-k_3)(c_2-c_3)(c_1-c_4)]\end{aligned} \tag{26f}$$

$$|A|C_{23} = c_3'(k_3+k_4)(k_1-k_3)(c_1-c_4) - k_3'(k_1+k_4)(c_3+c_4)(c_1+c_3) \tag{26g}$$

$$|A|C_{24} = -c_4'(k_3+k_4)(k_1+k_4)(c_1+c_3) + k_4'(k_1-k_3)(c_3+c_4)(c_1-c_4) \tag{26h}$$

$$|A|C_{31} = -c_1'(k_1+k_4)(k_1+k_2)(c_2+c_4) + k_1'(k_2-k_4)(c_1+c_2)(c_1-c_4) \tag{26i}$$

$$|A|C_{32} = c_2'(k_2-k_4)(k_1+k_2)(c_1-c_4) - k_2'(k_1+k_4)(c_1+c_2)(c_2+c_4) \tag{26j}$$

$$\begin{aligned}|A|C_{33} = {} & c_3'[(k_1+k_4)(k_2+k_3)(c_2+c_4) + (k_1-k_3)(k_2-k_4)(c_1-c_4)] \\ & + k_3'[(k_1+k_4)(c_1+c_3)(c_2+c_4) + (k_2-k_4)(c_2-c_3)(c_1-c_4)]\end{aligned} \tag{26k}$$

$$|A|C_{34} = -c_4'(k_1+k_4)(k_2-k_4)(c_1+c_2) - k_4'(k_1+k_2)(c_2+c_4)(c_1-c_4) \tag{26l}$$

$$|A|C_{41} = c_1'(k_1+k_2)(k_1-k_3)(c_2-c_3) - k_1'(k_2+k_3)(c_1+c_2)(c_1+c_3) \tag{26m}$$

$$|A|C_{42} = -c_2'(k_1+k_2)(k_2+k_3)(c_1+c_3) + k_2'(k_1-k_3)(c_1+c_2)(c_2-c_3) \tag{26n}$$

$$|A|C_{43} = -c_3'(k_1-k_3)(k_2+k_3)(c_1+c_2) - k_3'(k_1+k_2)(c_1+c_3)(c_2-c_3) \tag{26o}$$

$$\begin{aligned}|A|C_{44} = {} & c_4'[(k_1+k_4)(k_2+k_3)(c_1+c_3) + (k_1-k_3)(k_2-k_4)(c_2-c_3)] \\ & + k_4'[(k_2+k_3)(c_2+c_4)(c_1+c_3) + (k_1-k_3)(c_1-c_4)(c_2-c_3)].\end{aligned} \tag{26p}$$

The form of (26) is such that the effects of approximations and special cases can readily be seen. In the case of vertical propagation, we know that $c_1=c_2=c_3=c_4=1$, $c_i'=0$, and

$k_1=k_4=k_x$ and $k_2=k_3=k_0$. We thus get the simple form for the coupling matrix

$$C=\begin{bmatrix} \frac{k_x'}{2k_x} & 0 & 0 & -\frac{k_x'}{2k_x} \\ 0 & \frac{k_0'}{2k_0} & -\frac{k_0'}{2k_0} & 0 \\ 0 & -\frac{k_0'}{2k_0} & \frac{k_0'}{2k_0} & 0 \\ -\frac{k_x'}{2k_x} & 0 & 0 & \frac{k_x'}{2k_x} \end{bmatrix}. \tag{27}$$

From the above form of C we see that an upgoing ordinary wave is reflected into a downgoing ordinary wave and that an upgoing extraordinary wave is reflected into a downgoing extraordinary wave. We see that modes 1 and 3 propagate independently of modes 2 and 4.

In order to discuss other special cases and approximations for oblique incidence, it must be kept firmly in mind that modes 1 and 4 are propagating and modes 2 and 3 are nonpropagating or evanescent. In the light of our previous discussion, this means that cos θ in (5) must, upon reflection, undergo a change in sign.

A simple example is propagation in a plane perpendicular to the magnetic meridian. Under these conditions cos ϕ of (5) and (8) is zero, so that $c_1=c_4=c_x$, $k_1=k_4=k_x$, $c_2=c_3=c_0$, and $k_2=k_3=k_0$. As a result of these simplifications, the coupling matrix becomes

$$C=C^1+C^2$$

where

$$C^1=\begin{bmatrix} \frac{c_x'}{c_0+c_x} & \frac{-c_0'(k_x-k_0)}{2k_x(c_0+c_x)} & \frac{-c_0'(k_x+k_0)}{2k_x(c_0+c_x)} & 0 \\ \frac{-c_x'(k_0-k_x)}{2k_0(c_0+c_x)} & \frac{c_0'}{c_0+c_x} & 0 & \frac{-c_x'(k_x+k_0)}{2k_0(c_0+c_x)} \\ \frac{-c_x'(k_0+k_x)}{2k_0(c_0+c_x)} & 0 & \frac{c_0'}{c_0+c_x} & \frac{c_x'(k_x-k_0)}{2k_0(c_x+c_0)} \\ 0 & \frac{-c_0'(k_0+k_x)}{2k_x(c_0+c_x)} & \frac{c_0'(k_0-k_x)}{2k_x(c_0+c_x)} & \frac{c_x'}{c_0+c_x} \end{bmatrix},$$

and

$$C^2=\begin{bmatrix} \frac{k_x'}{2k_x} & 0 & 0 & -\frac{k_x'}{2k_x} \\ 0 & \frac{k_0'}{2k_0} & -\frac{k_0'}{2k_0} & 0 \\ 0 & -\frac{k_0'}{2k_0} & \frac{k_0'}{2k_0} & 0 \\ -\frac{k_x'}{2k_x} & 0 & 0 & \frac{k_x'}{2k_x} \end{bmatrix}. \tag{28}$$

The form (28) will be identical for the case of a vertical magnetic field and oblique propagation in any direction. We notice that C_2 has a form identical to that of (27) and that the effects of cross coupling between ordinary and extraordinary modes on oblique propagation in the plane perpendicular to the magnetic meridian are proportional to the rate of change of the cosine of the zenith angle of the phase normal.

In order to gain further insight into the properties of the coupling and thus the interaction of the various modes of propagation in a nonhomogeneous ionosphere, we shall calculate the values of k_j and c_j for a typical ionosphere. Figure 3 shows the electron density of a normal daytime ionosphere for middle latitudes along with a collision frequency. Daytime conditions are chosen so as not to impose too much of a violation on the quasi-longitudinal approximation. We shall also assume a constant magnetic field strength of 0.45×10^{-4} weber/m^2, a dip angle of 60 degrees, and a propagation frequency of 10 kc/s. The values of k_j and c_j as a function of altitude are computed from (1), (5), (8), and (13) and the magnitudes of k_j and c_j are shown in figure 4 (*a–h*) and the arguments in figure 5 (*a–h*) for several initial values of ψ and ϕ. Figures 4 and 5 show that the conditions imposed by propagation in a plane perpendicular to the magnetic meridian represent generally valid approximations for propagation in any direction because of the very small differences between c_1 and c_4, and c_2 and c_3.

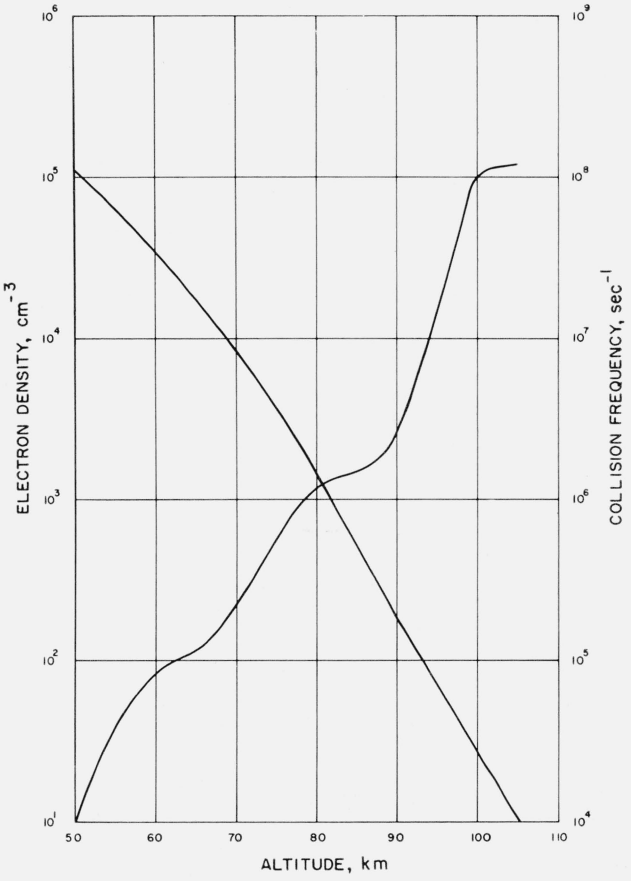

FIGURE 3. *Model ionosphere showing electron density and electron collision frequency.*

The second term in (28) is quite easy to interpret because it is made up of logarithmic derivatives of the propagation constant. Let us write $k_{0,x}$ in the form $|k_{0,x}|e^{i\gamma}$ where $|k|$ is the magnitude of k and γ is its argument, shown in figures 4 and 5, respectively. Then the nonzero matrix elements of C^2 in (29) may be expressed as

$$C^2_{ij}=1/2\ \ln'|k|+1/2\ i\,\gamma'_{0,x}. \tag{29}$$

Thus γ' is the slope of the curve on figure 5 (*a–h*) and $\ln'|k|$ is the slope of the curve shown in figure 4 (*a–h*) since $|k|$ is plotted on a logarithmic scale. Similarly $\frac{c'_{0,x}}{c_0+c_x}$ which appears in all the

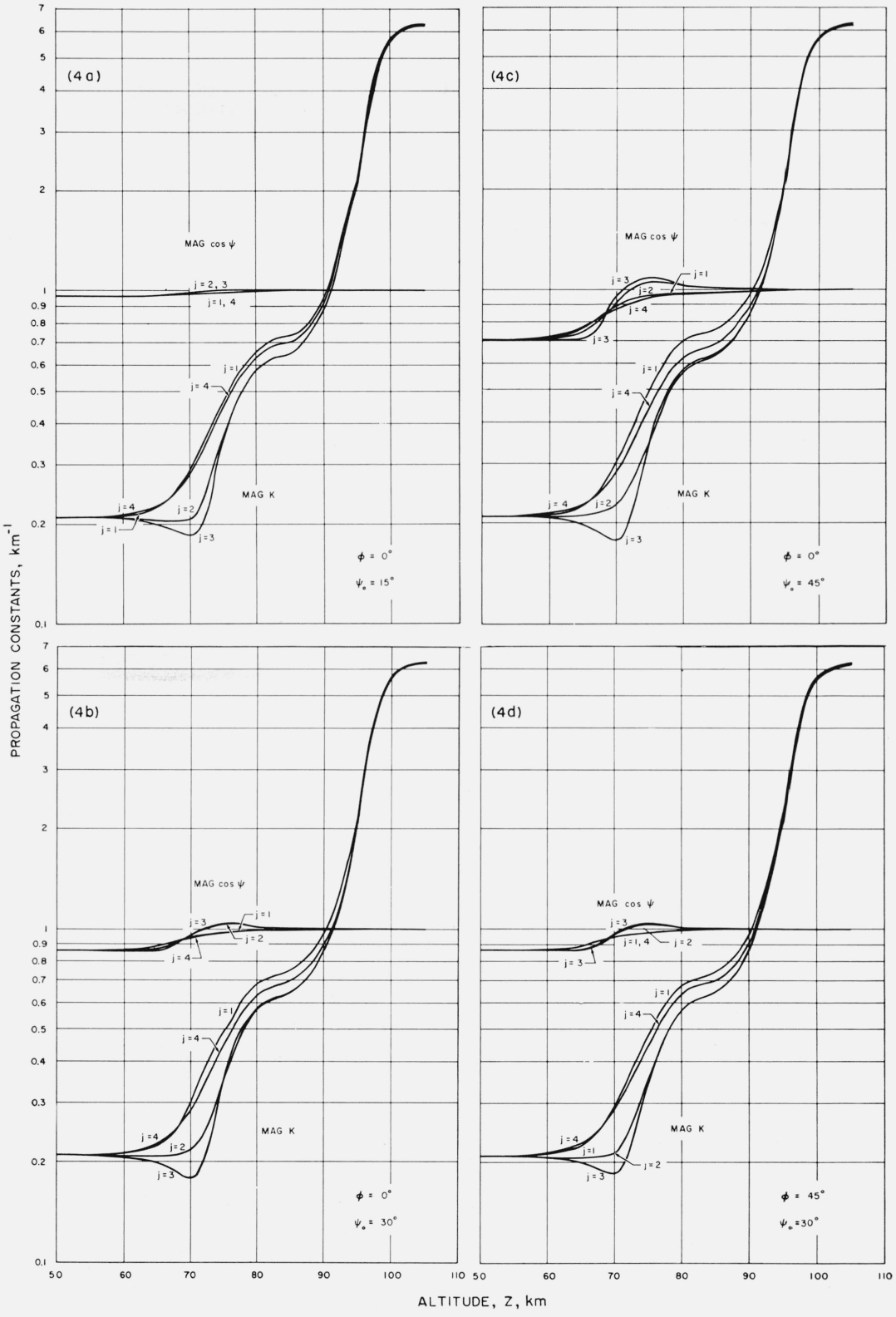

FIGURE 4. *Magnitude of the propagation constant and of cos ψ.*

648645—62——3

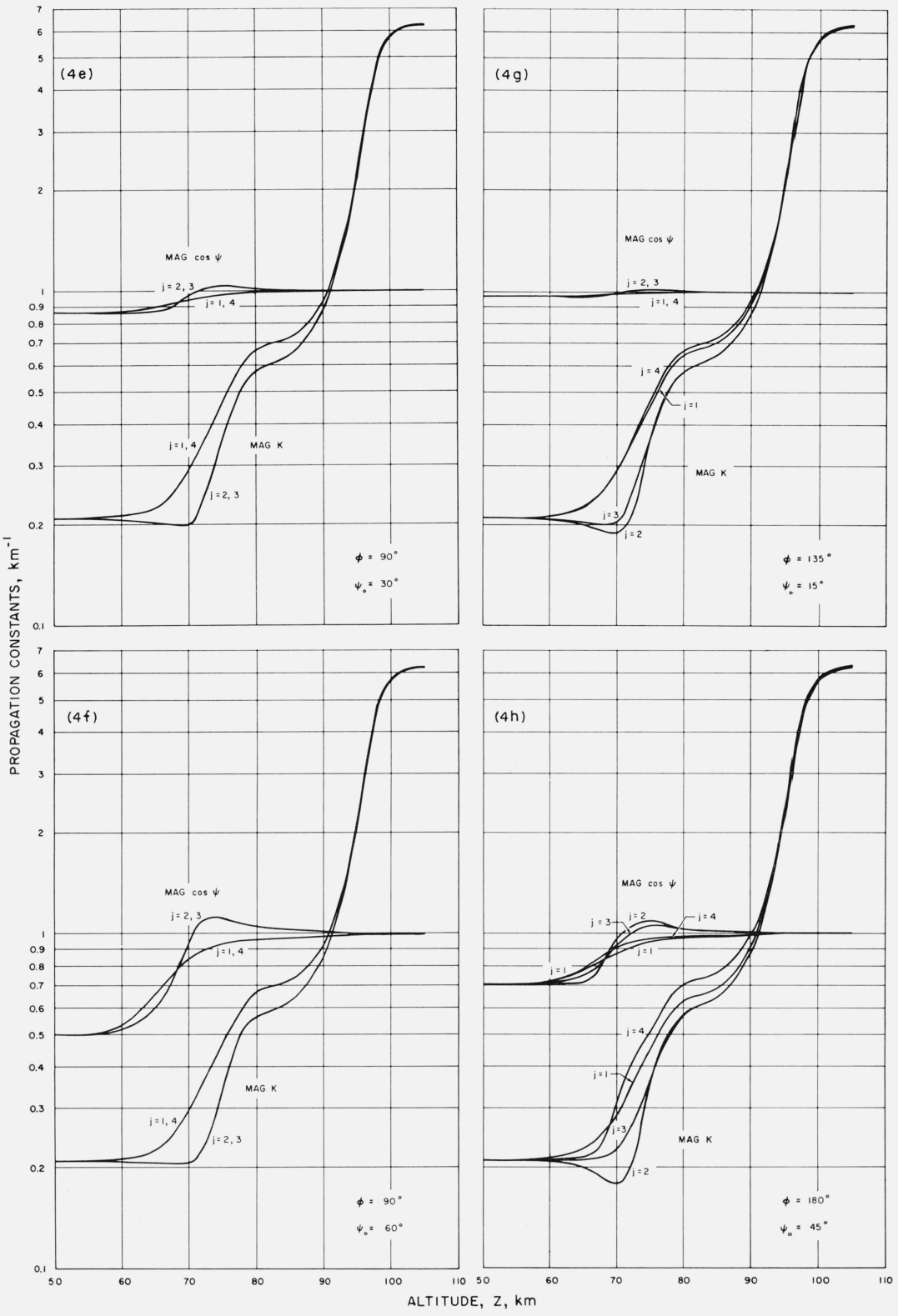

FIGURE 4.—Continued.

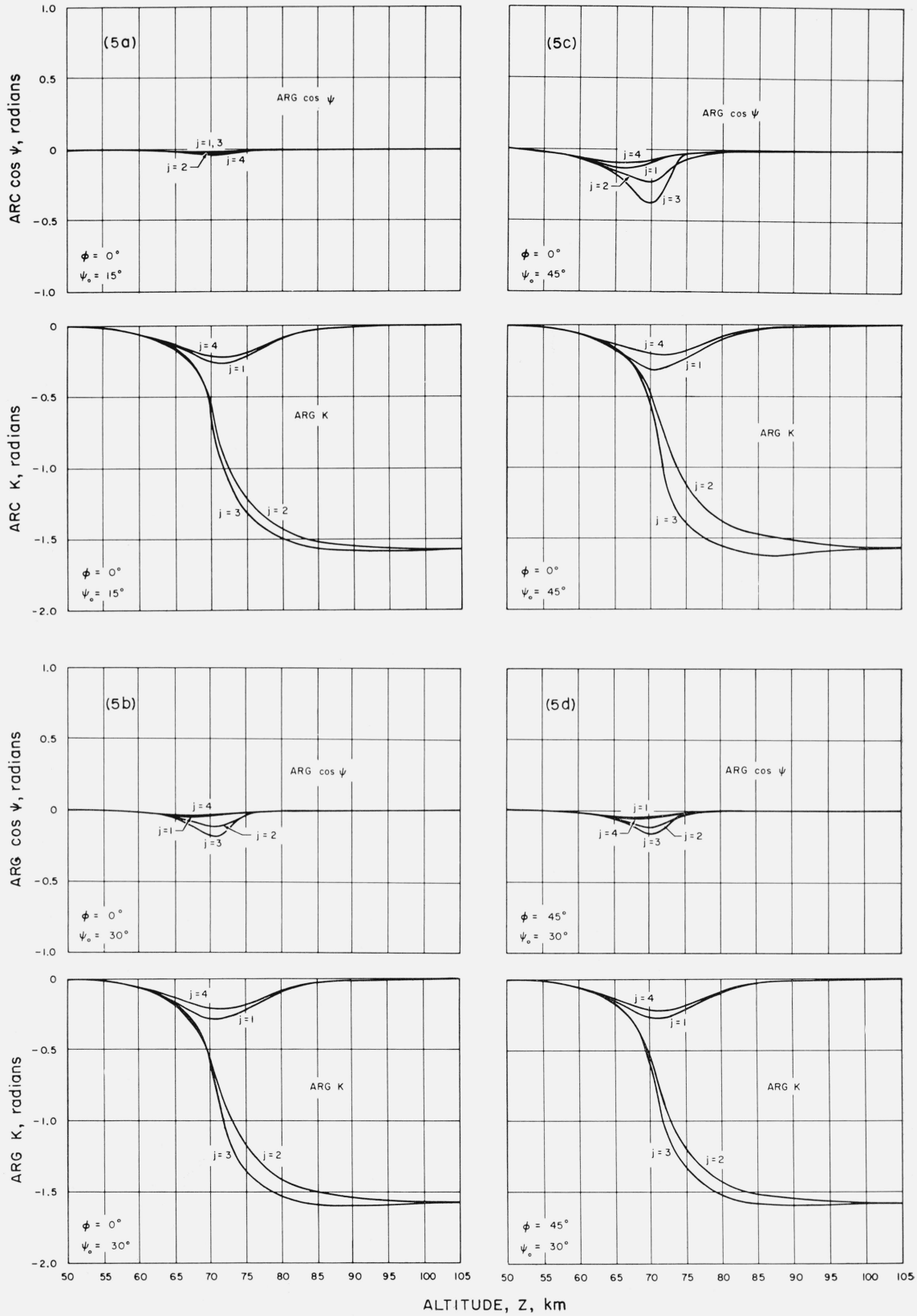

FIGURE 5. *Arguments of the propagation constant and of cos ψ.*

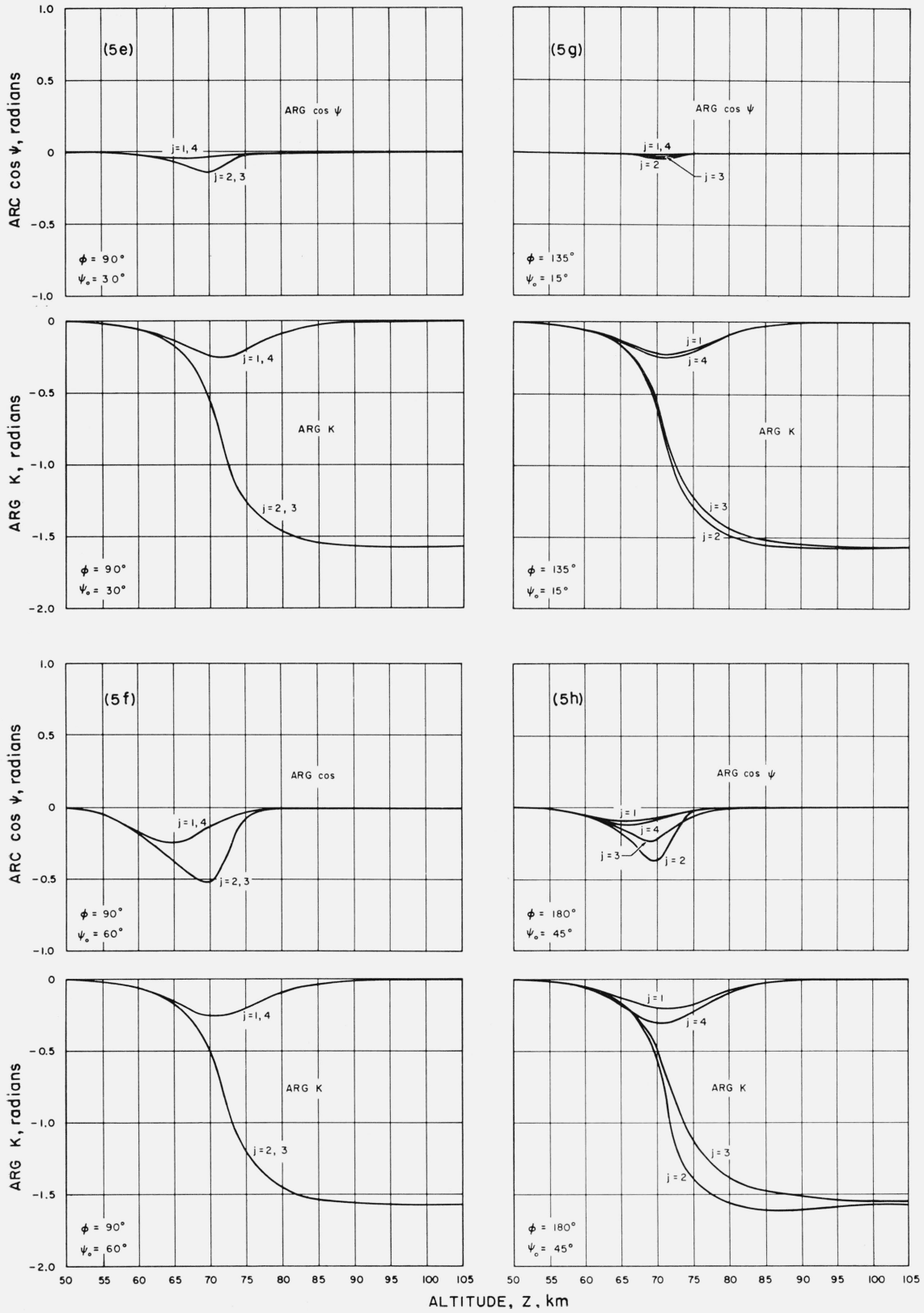

FIGURE 5.—Continued.

nonzero elements in C^1 of (28), may to a good approximation be written in the form

$$\frac{c'_{0,x}}{c_0+c_x} \simeq 1/2 \ln'|c|+1/2\, i\gamma'_c, \tag{30}$$

where γ_c is the argument of the cosines. Equation (30) is valid to within about 10 percent because the magnitudes and arguments of c_j are approximately equal.

The coupling that produces reflection between the two ordinary modes and between the two extraordinary modes is the strongest and also it is relatively independent of the angle of incidence from below the ionosphere. The coupling between modes 2 and 3 is stronger than between modes 1 and 4 because modes 2 and 3 undergo a large change in argument between the altitudes of 65 and 80 km.[1]

Cross-coupling terms shown in matrix C^1 are relatively weak except for highly oblique incidence. Factors of the type $\frac{k_0+k_x}{2k_{0,x}}$ have a magnitude that varies between 1 and $1/\sqrt{2}$ and an argument that varies between 0 and $\pi/4$. Thus terms representing coupling between modes 1 and 3, and modes 2 and 4 are characterized by the logarithmic derivative of the c's. However, reflective coupling due to the elements of C^1 occurs primarily between the altitude of 65 and 75 km, whereas reflective coupling due to the elements of C^2 is more in the 70 to 80 km range. Thus careful observation of the polarization of the reflected wave should allow observation of two different regions of the ionosphere.

Coupling between the two upgoing modes and two downgoing modes, represented by the matrix elements (C^1_{12}, C^1_{21}) and (C^1_{34}, C^1_{43}), contain factors of the type $(k_0-k_x)/2k_{0,x}$. The magnitude of this factor varies from zero at low altitudes, to $1/\sqrt{2}$ at high altitudes. Thus it is to be expected that coupling between the upgoing modes or between the downgoing modes be somewhat less than reflective coupling between ordinary and extraordinary modes.

4. Some Comments on the Conversion of Spherics Into Whistlers

As a wave penetrates the D region of the ionosphere, some of the wave energy is converted into other modes, which results in the process of reflection, while some of the energy is dissipated by electron collisions with the neutral particles. In order to obtain an estimate of how much a penetrating wave is attenuated, we shall compute the attenuation coefficients of the WKB solution of mode 1 given by

$$\boldsymbol{E}_1=\boldsymbol{E}_0 \exp\left[-i\int_0^z k_1 \cos\psi_1\, dz\right],$$

where the attenuation coefficient is given by

$$\exp-\left[\int_0^z \mathrm{Im}\,(k_1 \cos\psi_1)dz\right]$$

where Im (x) denotes the imaginary part of x. Table 1 shows some attenuation coefficients of mode 1 for several initial values of ψ and ϕ.

TABLE 1. *Attenuation of the WKB solutions for the upgoing propagating mode as a function of the angle of incidence*

Angles of incidence	Amplitude attenuation	Energy absorbed
deg	*Nepers*	*db*
ϕ=180 ψ=15	1.52	13.2
=180 =30	1.54	13.4
=180 =45	1.59	13.8
=180 =60	1.71	14.8
=180 =75	1.91	16.5
=135 =15	1.56	13.5
=135 =30	1.58	13.7
= 0 =15	1.72	14.9

[1] Figure 5 (*a–h*) is scaled such that a distance of one radian is the distance represented by a factor of e on figure 4 (*a–h*).

It can be seen from table 1 that the total absorption of, say a whistler signal, is relatively independent of the angle of incidence. It increases only gradually with increasing zenith angle. The favored azimuthal direction is in the same azimuth of the magnetic field. The optimum angle of incidence for minimum attenuation is somewhere between the zenith and the direction of the magnetic field. The small variation of total attenuation as a function of the zenith angle (much less than a sec ψ variation) results from the sharp change in the direction of the wave normal toward the zenith as the refractive index of the ionosphere increases.

Also, as indicated in the previous section, the conversion of mode 1 into the downgoing modes, 3 and 4, is somewhat less for more-nearly-vertical incidence. Therefore we may conclude with some reservation that the optimum direction for the penetration of very low frequency energy into the ionosphere is that of a nearly vertically-propagating wave; however, the angles of optimum penetration have a rather broad maximum.

The complete picture of the injection of whistler energy into the ionosphere must await the complete solution of the coupled equations shown in (22). However, from figure 4 (*a–h*) we see that, as far as the direction of the phase normal is concerned and regardless of the initial direction of the incident spheric signal on the ionosphere, the whistler is injected into the ionosphere with its phase normal propagating vertically upward. Therefore, once the electron density gradient above 105 km flattens out, the ray path as shown by Storey [1953] will have a direction given by

$$\tan \alpha \cong -\tfrac{1}{2} \cot \delta$$

where α is the zenith angle of the group velocity vector. Therefore the ray path will assume a direction between the zenith and the magnetic field direction above the E layer. Figure 6 shows some probable ray paths in the magnetic meridian generated by a lightning discharge. Since with a vertical dipole source most of the energy is radiated obliquely into the ionosphere and since reflection and absorption of mode 1 is not critically dependent upon the zenith angle of injection into the ionosphere, whistler sources may be quite distant from their apparent sources determined by tracing magnetic lines of force. Studies of whistler propagation [Helliwell and Morgan, 1959] have shown this to be the case.

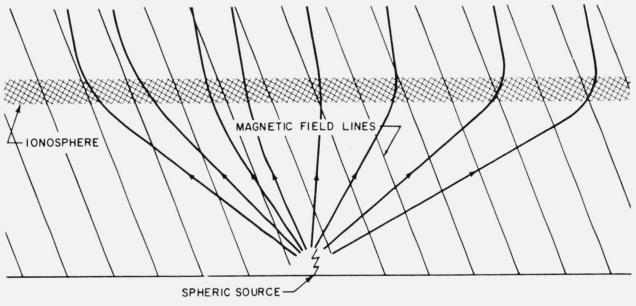

FIGURE 6. *Probable whistler ray paths through the ionosphere.*

5. Limitations on the Quasi-Longitudinal Approximation

The great simplifications made in the analysis were possible because the very-low-frequency wave was assumed to be circularly polarized. If this were not the case, then the matrix A would not have had its simple form, and its inverse would have been even more complicated so that the coupling matrix $A^{-1}A'$ would have been very difficult to analyze.

The condition that the quasi-longitudinal approximation be valid is that

$$|\beta|^2 = \frac{\omega_m^2 \sin^4 \theta}{4 \cos^2 \theta (\omega_p^2 + \nu^2)} \ll 1.$$

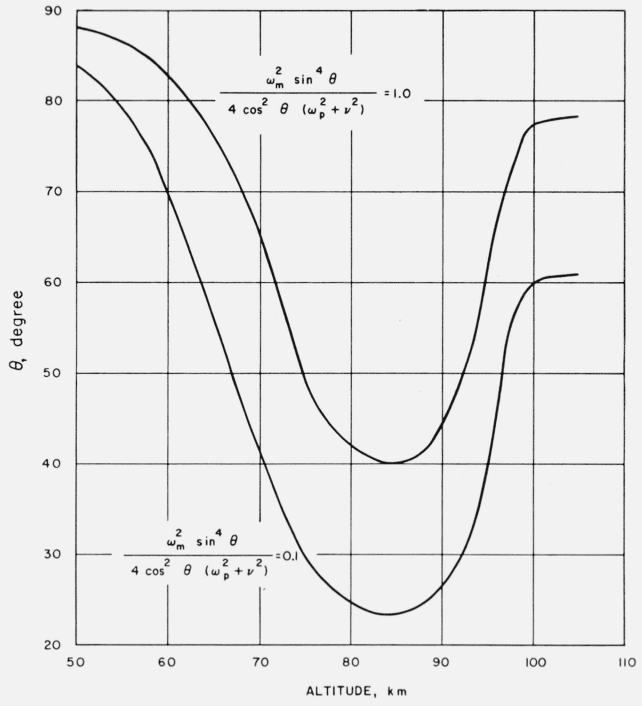

FIGURE 7. *Validity of the quasi-longitudinal approximation for the model ionosphere shown in figure 3.*

This condition is compatible with the requirement that $\cos\theta$ change sign on reflection. Figure 7 shows the angles θ for which $|\beta|^2=1$ and 0.1 computed from the model shown in figure 3.

It is seen that the quasi-longitudinal approximation becomes doubtful between 75 and 95 km with our present model ionosphere. At lower altitudes where the collision frequency is much greater than the gyrofrequency and at higher altitudes where the electron plasma frequency is greater than the gyrofrequency, the quasi-longitudianl approximation is useful. Since daytime reflection of VLF radio waves usually occurs below 75 km [Bracewell et al., 1951] and since most of the absorption occurs below 75 km, this analysis is useful for a qualitative discussion of these effects.

At altitudes around 85 km the breakdown in the quasi-longitudinal approximation is somewhat more serious. For here $|\beta|^2=0.6$ for vertical propagation. However, it can be seen from figures 4 and 5 that the elements in the coupling matrix C are small in this altitude range, so the accumulative effect of the error would not be too great.

Caution should be used in treating cases with highly oblique propagation, however; the quasi-longitudinal approximation is improved by the fact that as the wave propagates beyond 70 km, its wave normal becomes more vertical. This analysis would break down rather badly using a nighttime model ionosphere because there would be a wide range of altitudes at which the quantity $\frac{\omega_m^2}{\nu^2+\omega_p^2}$ would be considerably greater than unity. However, during times of enhanced D-region ionization produced by solar flares, auroral, and PCA events, the quasi-longitudinal approximation is more generally applicable. Also at higher geomagnetic latitudes where the magnetic field is closer to the vertical, the usefulness of quasi-longitudinal approximation is improved.

I thank Miss Estelle Guilbault for her able assistance in carrying out the numerical computations.

This work was supported by the U.S. Air Force Cambridge Research Laboratories under contract AF19(604)–8058.

6. Appendix. List of Symbols

A =matrix [see eq (20)]
A' =derivative of the matrix A
a^i_{jk} =[see eq (11)]
B_0 =magnetic induction of the earth's field
C =coupling matrix=$A^{-1}A'$
C^1 =coupling matrix [see eq (29)]
C^2 =coupling matrix [see eq (29)]
C_{ij} =element of C
c =velocity of light
c =cosine of zenith angle
E =electric field strength
$\boldsymbol{E}$ =$E \exp(-ik \cos \psi z)$
e =electronic charge
e =base of natural logarithm
f =propagation frequency
k =propagation constant
m =electron mass
N_e =electron density
Q =diagonal matrix of elements $k_j \cos \psi_j$
z =altitude
α =angle between phase normal and ray direction
δ =dip angle of magnetic field
ϵ =integer function
θ =angle between direction of propagation and magnetic field
ψ =zenith angle of phase normal
ν =electron collision frequency
ϕ =azimuthal angle of phase normal
γ =phase angle
ω =$2\pi f$ angular frequency
$\omega_p^2=\dfrac{e^2N_e}{\epsilon_0 m}$ square of electron plasma angular frequency
ω_m =electron gyrofrequency
$\vec{1}_k$ =unit vector in direction of phase normal
$\vec{1}_b$ =unit vector in direction of magnetic field
$\vec{1}_{y'}$ =unit vector to specify polarization of electric field (see fig. 1)
$\vec{1}_{z'}$ =unit vector to specify polarization of electric field (see fig. 1)

7. References

Barron, D. W., and K. G. Budden, The numerical solution of differential equations governing reflection of long radio waves from the ionosphere III, Proc. Roy. Soc. **A249,** p. 387 (1959).

Bracewell, R. N., K. G. Budden, J. A. Ratcliffe, T. W. Straker, and K. Weeks, The ionospheric propagation of long and very long radio waves over distances less than 1000 km, Proc. Inst. Elec. Engrs. (London) **98,** pt. III, 221 (1953).

Budden, K. G., Radio waves in the ionosphere, p. 398 (Cambridge University Press, 1961).

Helliwell, R. A., and M. G. Morgan, Atmospheric whistlers, Proc. IRE **47,** No. 2, 200 (1959).

Johler, J. R., and J. D. Harper, Jr., Reflection and transmission of radio waves at a continuously stratified plasma with arbitrary magnetic induction, J. Research NBS **66D** (Radio Prop.) No. 1, 81–99 (Jan.–Feb. 1962).

Storey, L. R. O., Investigation of whistling atmospherics, Phil. Trans. Roy. Soc. **1,** 246 (1953).

Wait, J. R., Terrestrial propagation of VLF radio waves—a theoretical investigation, J. Research NBS **64D** (Radio Prop.) No. 2, 153 (Mar.–Apr. 1960).

(Paper 66D6–226)